Evaluation of Trap Signatures in Fe-doped 0.12 μm InAlN/GaN HEMTs by DCT, Y22 and Y21 Techniques

P. Vigneshwara Raja, Emmanuel Dupouy, Raphaël Sommet, Jean-Christophe Nallatamby

Evaluation of Trap Signatures in Fe-doped 0.12 µm InAlN/GaN HEMTs by DCT, Y_{22} and Y_{21} Techniques

P. Vigneshwara Raja[1], Emmanuel Dupouy[2], Raphaël Sommet[2], Jean-Christophe Nallatamby[2]
[1]Department of Electrical Engineering, IIT Dharwad, Karnataka - 580011; email: vigneshwararaja@iitdh.ac.in
[2]XLIM Laboratory, CNRS UMR 7252, University of Limoges, F-19100 Brive, France.

***Abstract*—**Electrically active defects in 0.12 µm InAlN/GaN high-electron mobility transistors (HEMTs) with Fe-doped buffer are extensively analyzed by drain current transient (DCT), output and forward-transfer admittance (Y_{22} and Y_{21}) parameters. The DCT, Y_{22}, and Y_{21} properties are measured at several temperatures (30 °C to 165 °C) to determine the trap parameters using Arrhenius analysis. The measurements are also performed at two distinct drain voltage conditions to quantify the field-assisted (Poole-Frenkel) carrier emission effect on the trap activation energy. All these defect characterizations indicate the Fe-related acceptor trap in the buffer, however each technique yields quite different energies (E_C – 0.62 to E_C – 0.43 eV), and capture cross-sections (5×10^{-15} cm^2 to 6×10^{-17} cm^2). A shallow trap at E_C – 0.13 eV is identified from Y_{21}, which is attributed to the surface trapping. This work is an essential initial step toward estimating the zero-field (actual) activation energy of a trap, by quantitatively incorporating the electric field effects on the emission rate.

I. Introduction

The compensational iron (Fe) dopants are purposely introduced during layer growth of GaN buffer, to achieve effective 2DEG confinement, reduced vertical buffer leakage current, and higher breakdown voltage for GaN-based HEMTs. Despite these advantages, the Fe-doping creates deep-level acceptor traps in the buffer layer. The electron trapping in the buffer causes a transient reduction in RF output power, power added efficiency (PAE) and current collapse effects. Therefore, electrically active traps present in the GaN-based HEMTs need to be identified to improve the epilayer quality. Relative to AlGaN/GaN HEMT technology, the InAlN/GaN HEMTs are more attractive for RF and microwave applications due to their superior properties such as lattice-matched heterointerface, thin InAlN barrier, high spontaneous polarization, and absence of inverse piezoelectric effect. Extensive research studies were carried out to characterize deep-level traps in the AlGaN/GaN HEMTs. On the other hand, limited reports are available in the literature on detecting the traps in the lattice-matched InAlN/GaN-based HEMTs. For this reason, InAlN/GaN HEMT with Fe-doped buffer is selected for this study.

Drain current transient (DCT) spectroscopy, and output admittance parameters (Y_{22}) are the widely used methods to identify the deep-level traps in the GaN-based HEMTs [1]-[5]. In this work, double pulsed DCT spectroscopy and Y_{22} parameters are measured at two distinct drain voltages to quantify the Poole-Frenkel (field-assisted carrier emission) effect on the emission time constants; and the corresponding change in the trap activation energy is analyzed. So, this report is an essential initial step for estimating the zero-field (actual) trap activation energy, by quantitatively including the field effects on the emission rate. A careful calibration procedure is always necessary to conduct reliable Y_{21} experiments, compared to the Y_{22} measurements. Due to this practical difficulty, many authors [1], [4] applied Y_{22} parameters to characterize the traps in the HEMT. Benvegnu *et al.* [3] detected two traps at 0.61 eV and 0.25 eV using Y_{21} measurements, but their device is AlGaN/GaN HEMT. In this work, Y_{21} parameters of InAlN/GaN HEMT are measured at two different bias conditions, and the trap signatures are computed. The trapping influences on the pulsed I-V characteristics of InAlN/GaN HEMTs are investigated. Therefore, this paper reports the comprehensive trap characterization of the Fe-doped 0.12 µm InAlN/GaN HEMTs by pulsed I-V, DCT, Y_{22}, and Y_{21} properties.

II. Experiment

The lattice-matched $In_{0.17}Al_{0.83}N$/GaN heterostructure was grown on a silicon carbide substrate. The heteroepitaxial layer includes 2 µm of Fe-doped GaN buffer layer, undoped GaN channel layer, 10 nm InAlN barrier layer, and thin GaN cap layer. The HEMT features an ultra-short gate length of 0.12 µm, and a gate width of 50 µm with six fingers (size 6×50 µm). The source terminated field plate and silicon nitride passivation were integrated with the transistor structure.

The pulsed I-V measurements were conducted at several quiescent bias points (V_{GSQ}, V_{DSQ}) to inspect the trapping effects in the HEMT. The DCT and *Y*-parameter characterization procedures are reported elsewhere [1], [5]. As a first step in the DCT, the traps in the HEMT were populated by synchronously pulsing the gate and drain voltages to a deep off-state bias condition (V_{GF}, V_{DF}) = (-6 V, 10 V) for 1 ms pulse width. At the end of the filling pulse, the HEMT was instantaneously switched to a semi-on bias point (V_{GM}, V_{DM}), and the emission transient due to the charge detrapping was measured in the time range of 1 µs to 10 s. The DCT spectroscopy was acquired at various operating temperatures from 30 °C to 165 °C.

Before the Y_{22} and Y_{21} experiments, the standard short-open-load-through (SOLT) practice was employed to calibrate the

vector network analyzer. The Y_{22} and Y_{21} parameters were measured at a fixed on-state gate and drain bias voltages in the low-frequency range of 100 Hz to 10 MHz. The Y_{22} and Y_{21} measurements were performed at several temperatures (30 °C to 165 °C) to compute the trap parameters from the Arrhenius plot. The DCT, Y_{22}, and Y_{21} experiments were also conducted at two different drain voltages to evaluate the field-assisted carrier emission effect on the trap activation energy.

III. Results and Discussion

The threshold voltage of -2 V and peak transconductance of 0.5 S/mm are extracted from the I_{DS}-V_{GS} properties of Fe-doped InAlN/GaN HEMT. Figure 1 shows the pulsed I_{DS}-V_{DS} of the HEMT at various quiescent bias points (V_{GSQ}, V_{DSQ}). The pulse width and period are 500 ns (T_{ON}), and 500 ms (T_{period}), respectively. The pulsed I_{DS}-V_{DS} at (V_{GSQ}, V_{DSQ}) = (0 V, 0 V) is considered as the reference characteristic, since negligible trapping is anticipated at this bias condition. The positive drain quiescent bias voltage (V_{GSQ}, V_{DSQ}) = (0 V, 10 V) may induce electron trapping in the gate-drain access region (known as drain-lag), as a result, a reduction in drain current (I_{DS}) is noticed. The drain current also decreases upon exposure to the negative gate quiescent bias (V_{GSQ}, V_{DSQ}) = (-7 V, 0 V), due to the trapping under gate and drain-side of the gate-edge regions (gate-lag effect). The profound off-state quiescent bias voltage (V_{GSQ}, V_{DSQ}) = (-7 V, 10 V) promotes a strong electron trapping under gate and gate-drain access regions (reverse biased G-D voltage V_{GDQ} = -17 V), so a significant reduction in I_{DS} is observed for this case. The pulsed I-V characteristics reveal the presence of trapping in the HEMT [2]. However, the trap parameters cannot be identified from the pulsed I-V.

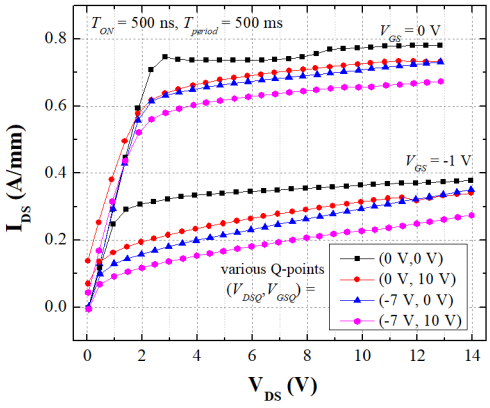

Fig. 1. Pulsed I_{DS}-V_{DS} characteristics of Fe-doped InAlN/GaN HEMT at various quiescent bias points (V_{GSQ}, V_{DSQ}).

Figure 2(a) depicts the DCT spectroscopy measured at V_{GM} = -1.6 V, V_{DM} = 1 V for several temperatures (30 °C to 165 °C). The DCT data is fitted by the multi-exponential function [1] and the computed derivative spectra for the fitted DCT are plotted in Fig. 2(a). The positive peak (T1) in the DCT derivative spectra indicates the existence of a trap in the HEMT [1], [2]. The emission time constant of the trap (T1) is extracted from the peak position. It is seen that the emission time constant (τ_n = 54 ms at 30 °C, 1 ms at 90 °C, and 22 µs at 165 °C) decreases with increasing temperature as per the Arrhenius law.

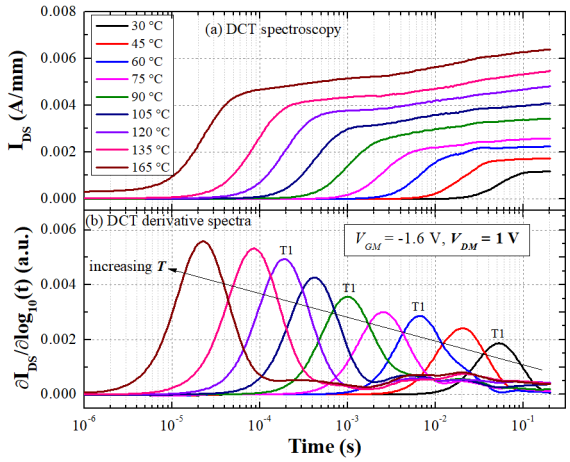

Fig. 2. (a) DCT spectroscopy of the HEMT measured at V_{GM} = -1.6 V, V_{DM} = 1 V. (b) Corresponding DCT derivative spectra at several temperatures (30 °C to 165 °C).

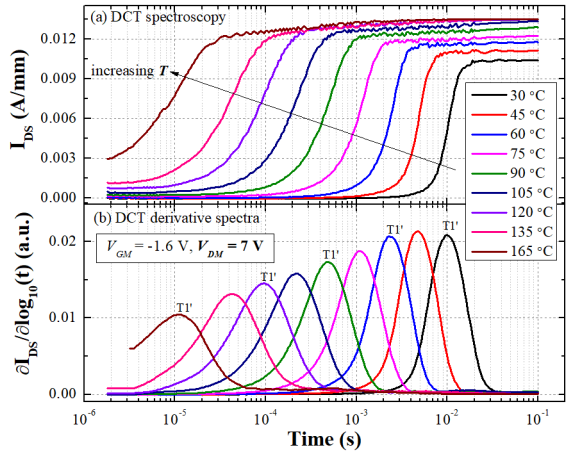

Fig. 3. (a) DCT spectroscopy measured at V_{GM} = -1.6 V, V_{DM} = 7 V. (b) DCT derivative spectra at various temperatures (30 °C to 165 °C).

Figures 3(a) and (b) display the DCT spectroscopy and the corresponding derivative spectra acquired at the bias point of V_{GM} = -1.6 V, V_{DM} = 7 V for various temperatures (30 °C to 165°C). A similar trapping phenomenon T1' is detected in Fig.3. The DCT derivative spectra at two different drain bias voltages (V_{DM} = 1 V and 7 V) are compared in Fig. 4(a). The DCT signal amplitude for V_{DM} = 1 V case is found to be higher than its counterpart (V_{DM} = 7 V); the observed variation in the signal magnitude is due to the chosen I_{DS} range while measuring the emission transient of the DCT; please refer to the I_{DS} values in Figs. 2(a) and 3(a). It is clearly visualized in Fig. 4(a) that the emission time constant decreases (54 ms at V_{DM} = 1 V, 10 ms at V_{DM} = 7 V for 30 °C) upon increasing the drain voltage at each temperature. In general, two physical mechanisms may accelerate the carrier emission rate: (1) Poole-Frenkel (PF) emission effect and (2) device self-heating [1]-[5]. Note that, HEMT devices are developed on silicon carbide substrate (which has high thermal conductivity) and the lower drain bias voltages ($V_{DM} \leq 7$ V) are adopted during the DCT emission transient. This indicates that the self-heating effects are negligible in the HEMT at the selected bias range. Therefore, the field-assisted PF carrier emission is responsible for the

decrease in the emission time constant with the drain voltage. The temperature-dependent DCT properties are related to activation energy (E_a) and capture cross-section (σ_n) of the trap based on the Arrhenius equation [1]:

$$\ln(\tau_n T^2) = E_a / kT - \ln(\sigma_n v_{th} N_C / g T^2) \qquad (1)$$

where T is the temperature, g is the degeneracy factor, v_{th} is the carrier thermal velocity, k is the Boltzmann's constant, N_C is the effective density of states in the conduction band. Figure 4(b) shows $ln\ (\tau_n T_2)$ vs. $1/kT$ Arrhenius plot for T1 and T1' constructed from the DCT spectroscopy. E_a and σ_n for the traps T1 (0.6 eV, 4×10^{-15} cm^2) and T1' (0.53 eV, 1.5×10^{-15} cm^2) are computed from the slope and intercept of the Arrhenius plot. Thus, the trap activation energy of T1 is underestimated at the high drain voltage (V_{DS} = 7 V) due to the PF carrier emission. As the drain voltage increases in the HEMT, the accelerating electric field along the channel upsurges, as a consequence, the trapped electrons require relatively lesser activation energy for thermal emission (detrapping). The electric field (F) induced potential barrier lowering ($\Delta\phi_{PF}$) effect and the corresponding reduction in the thermal activation energy $E_i(F)$ can be parameterized as per the expression [4]:

$$E_i(F) = E_i(0) - \Delta\phi_{PF} = (q/\pi\varepsilon)^{1/2}\sqrt{F} = \beta\sqrt{F} \qquad (2)$$

where $E_i(0)$ is the zero-field activation energy of the trap (ionization energy of the trap in the absence of electric field), q is the electric charge, ε is the dielectric constant. Hence, it is recommended to perform trap characterization experiments at lower drain voltages to determine the actual activation energy. Suppose, if emission time constant variations are linearly correlated with the applied electric field changes through the simulation model, then the zero-field trap activation energy can be identified. Hence, this work is an essential initial step for estimating zero-field activation energy before developing the physical simulation model. Our earlier reports [1], [5] indicate that the positive peak in the DCT derivative spectra corresponds to the electron detrapping process from the trap positioned at $E_C - E_T$. Accordingly, the energy location of the trap T1 and T' is considered at E_C – 0.6 eV and E_C – 0.53 eV.

Figure 5 shows the low-frequency (LF) Y_{22} parameters measured at two bias points (a) V_{GS} = -1.6 V, V_{DS} = 1 V and (b) V_{GS} = -1.6 V, V_{DS} = 7 V in the temperature range of 75 °C to 165 °C. The imaginary part of the Y_{22} peak frequency (f_p) is related to the emission time constant (τ_n) as $f_p = 1/2\pi\tau_n$ [4]. The Y_{22} peak position (T1* and T1**) moves to high frequency with the temperature due to the increased emission rate. Because of the field-assisted electron (PF) emission behavior, the emission rate accelerates with the increasing drain voltage, referring to the Y_{22} peak positions noted at two V_{DS} conditions in Figs. 5(a) and (b). Figure 6 displays the Arrhenius plots for T1* and T1** constructed from Y_{22}. E_a (0.58 eV) and σ_n (7×10^{-15} cm^2) for T1* are computed from the Arrhenius plot for V_{DS} = 1 case; this activation energy of T1* is lower than that calculated from the DCT even at similar drain voltages. Thus, deviation in activation energy is observed between these two measurements (DCT and Y_{22}) conducted at identical bias conditions. The trap activation energy of T1** (0.5 eV, 4×10^{-15} cm^2) is further undervalued due to the field-induced potential barrier lowering effect at the high drain bias point of V_{GS} = -1.6 V and V_{DS} = 7V.

Our earlier simulation results reveal that the Y_{22} frequency dispersion properties are more sensitive to the buffer traps, suggesting that the electron traps T* at E_C - 0.58 eV and T** at E_C - 0.5 eV are located in the GaN buffer. In fact, the traps (T1, T', T*, T**) deduced from DCT and Y_{22} are linked to the Fe-related acceptor traps (E_C – 0.6 eV to E_C – 0.5 eV).

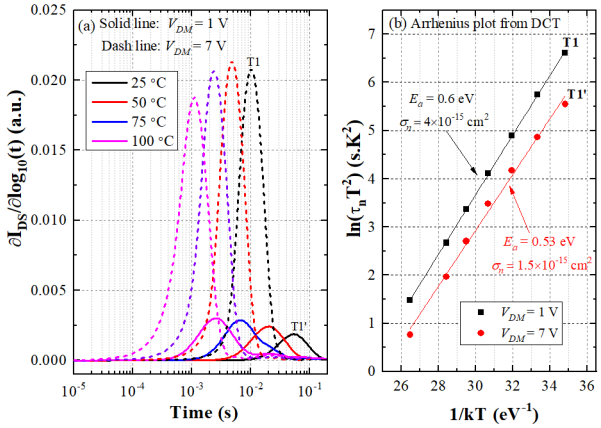

Fig. 4. (a) DCT derivative spectra at two different drain bias conditions (V_{DM} = 1 V and 7 V) are compared. (b) Arrhenius plot for the traps T1 and T1' identified from the DCT spectroscopy.

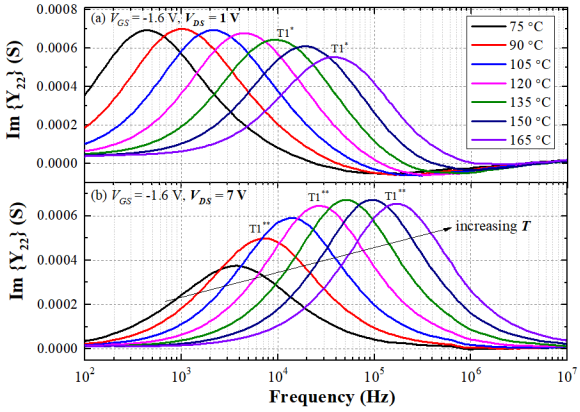

Fig. 5. Low-frequency (LF) Y_{22} parameters measured at two different bias points (a) V_{GS} = -1.6 V, V_{DS} = 1 V and (b) V_{GS} = -1.6 V, V_{DS} = 7 V in the temperature range of 75 °C to 165 °C.

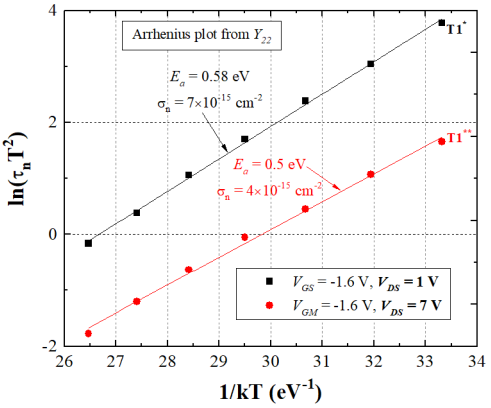

Fig. 6. Arrhenius plots for the traps T1* and T1** deduced from Y_{22} characteristics at two different drain voltage conditions.

The temperature-dependent (45 °C to 150 °C) LF Y_{21} properties at V_{GS} = -1.62 V, V_{DS} = 1 V are plotted in Fig. 7. Unlike Y_{22} spectra, both negative (T1$^{\#}$) and positive (T2) peaks are identified in Y_{21} spectra, supporting the observations of Benvegnu *et al.* [3]. Both peaks shift towards higher frequencies with the temperature, so that the emission rate of the traps follows the Arrhenius temperature dependence. E_a and σ_n for the traps T1$^{\#}$ (0.43 eV, 5.5×10^{-17} cm^2), and T2 (0.13 eV, 5×10^{-19} cm^2) are calculated from the Arrhenius plots displayed in Fig. 8. In TCAD simulation, T1$^{\#}$ is considered as an electron trap at E_C – 0.43 eV and is located in the GaN buffer; the simulated Y_{21} spectra closely track with the negative peak T1$^{\#}$ in Fig. 7 (not shown). It should be noted that the buffer trap produces a positive peak in Y_{22}, while the same induces a negative peak in Y_{21}. Hence, the simulation results reveal that the trap T1$^{\#}$ at E_C – 0.43 eV is related to the Fe-related acceptor states in the buffer. In this work, various trap characterization techniques detect the Fe-related acceptor trap energies from E_C – 0.62 eV to E_C – 0.43 eV. Placing the trap T2 (E_C – 0.13 eV) at the GaN/nitride interface in the simulation, can reproduce the positive peak in the Y_{21} spectra. Accordingly, the shallow trap T2 at E_C – 0.13 eV is attributed to the surface trap.

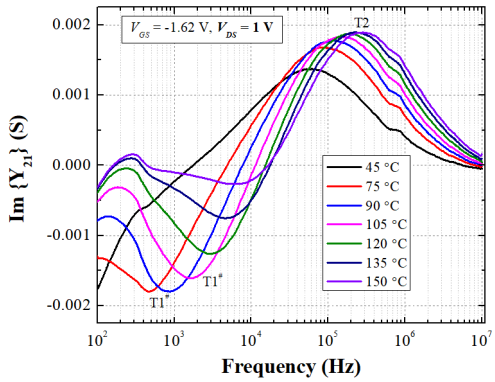

Fig. 7. Temperature dependent (45 °C to 150 °C) LF Y_{21} properties at V_{GS} = -1.62 V, V_{DS} = 1 V show two traps T1$^{\#}$ at 0.42 eV and T2 at 0.13 eV.

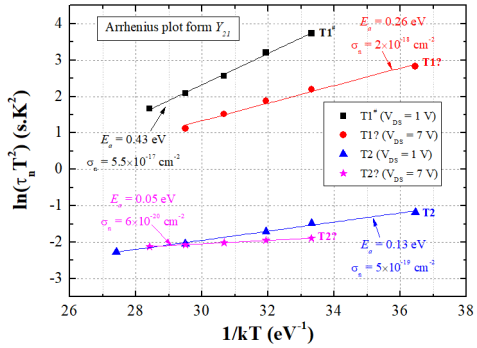

Fig. 8. Arrhenius plots for the traps T1$^{\#}$, T1?, T2, and T2?, identified from LF Y_{21} characteristics at two different bias points.

The Y_{21} properties measured at the high drain bias point of V_{GS} = -1.79 V, V_{DS} = 7 V are plotted in Fig. 9. A weak temperature dependence is noticed for both peaks; thereby significantly lower E_a and σ_n are identified for negative (0.26 eV, 2×10^{-18} cm^2) and positive (0.05 eV, 6×10^{-20} cm^2) peaks. This creates a dilemma of whether the negative peak (T1?) is associated with the Fe-related acceptor or not (likewise query arises for the negative peak (T2?) related to the surface trap), which remains an open question. Nevertheless, one point is clear that the LF Y_{21} frequency dispersion properties strongly depend on the operating bias condition. It is preferable to conduct Y_{21} measurements at a low drain voltage to acquire reliable data. The trap parameters identified from the various trap characterization methods are summarized in Table I.

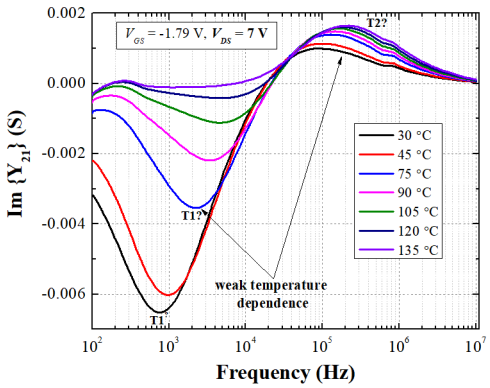

Fig. 9. LF Y_{21} properties measured at the high drain bias point of V_{GS} = -1.79 V, V_{DS} = 7 V for various temperatures (30 °C to 135 °C).

Table I. Summary of trap parameters deduced from various techniques.

Method	Bias point	Label	E_a (eV)	σ_n (cm^2)
DCT	V_{DS} = -1.6 V, V_{DS} = 1 V	T1	0.6	4×10^{-15}
	V_{DS} = -1.6 V, V_{DS} = 7 V	T1'	0.53	1.5×10^{-15}
LF Y_{22}	V_{DS} = -1.6 V, V_{DS} = 1 V	T1*	0.58	7×10^{-15}
	V_{DS} = -1.6 V, V_{DS} = 7 V	T1**	0.5	4×10^{-15}
LF Y_{21}	V_{DS} = -1.62 V, V_{DS} = 1 V	T1$^{\#}$	0.43	5.5×10^{-17}
		T2	0.13	5×10^{-19}
	V_{DS} = -1.79 V, V_{DS} = 7 V	T1?	0.26	2×10^{-18}
		T2?	0.05	6×10^{-20}

IV. Conclusion

The electrically active traps in Fe-doped InAlN/GaN HEMTs are comprehensively analyzed by pulsed I-V, DCT, Y_{22} and Y_{21}. The various trap characterization methods detect the Fe-related acceptor energies from E_C – 0.6 eV to E_C – 0.43 eV. The emission rate accelerates with the increasing drain voltage due to the field-assisted carrier emission, as a result the trap activation energy is underestimated from the Arrhenius calculation at higher drain voltages. A shallow trap at E_C – 0.13 eV identified by Y_{21}, is ascribed to the surface trap. Hence, it is shown that surface traps can be identified by means of Y_{21} frequency dispersion properties.

References: [1] P. V. Raja et. al. IEEE TED, vol. 67, pp. 2304, 2020, [2] D. Bisi et. al. IEEE TED, vol. 60, pp. 3166, 2013, [3] A. Benvegbu et. al. Int. J. Microw. Wirel. Technol., vol. 8 pp. 663, 2016, [4] C. Potier et. al. Int. J. Microw. Wirel. Technol., vo. 7, pp. 287, 2015, [5] P.V. Raja et.al. IEEE TED, vol. 69, pp. 4864, 2022.